Computer Simulation of a Three-phase Brushless Self-Excited Synchronous Generator

Vlatko Cingoski, Mitsuru Mikami and Hideo Yamashita
Faculty of Engineering, Hiroshima University, 1-4-1 Kagamiyama, Higashihiroshima 739-8527, Japan

Kenji Inoue
Faculty of Engineering, Hiroshima Institute of Technology, Hiroshima 731-5143, Japan

Reprinted from
IEEE TRANSACTIONS ON MAGNETICS
Vol. 35, No. 3, May 1999

Computer Simulation of a Three-phase Brushless Self-Excited Synchronous Generator

Vlatko Čingoski, Mitsuru Mikami and Hideo Yamashita
Faculty of Engineering, Hiroshima University, 1-4-1 Kagamiyama, Higashihiroshima 739-8527, Japan

Kenji Inoue
Faculty of Engineering, Hiroshima Institute of Technology, Hiroshima 731-5143, Japan

***Abstract*—Computer simulation of the operating characteristics of a three-phase brushless synchronous generator with self-exciter is presented. A voltage driven nonlinear time-periodic FEA is utilized to compute accurately the magnetic field distribution and the induced voltages and currents simultaneously. A method for numerical modeling of the diodes is also discussed. First, the computation procedure is briefly addressed, followed by the comparison between computed results and the experimental ones. The agreement between results is very good verifying the computational approach.**

***Index terms*— Electromagnetic transient analysis, rotating machine nonlinear analysis, brushless rotating machines, synchronous generator transient analysis, diode, finite element method.**

I. Introduction

Development of various electromagnetic devices with desired shape and operating parameters is usually a very time consuming and laborious task. Besides the intensive mathematical calculation, the development of a prototype device and performing a set of experimentations must be done before the optimal design is achieved. With the increased usage of semiconductor devices and permanent needs for easy and reliable speed, torque, voltage and current on-line control, a typical 2-D or even a 3-D FEA is not sufficiently accurate for the design of the modern electrical machines. Therefore, recently with the increase of the computer performances and resources, designers are more interested how to accurately simulate the operating conditions of such devices instead of building a machine prototype and testing it. For such simulations, new and more sophisticated methods and procedures must be employed [1], [2].

This paper deals with the numerical simulation of the operating characteristics of a 3-phase brushless self-exciting synchronous generator [3]. To accurately predict and investigate the influence of various electrical parameters, and due to complexity of generator's configuration which includes several windings, rectifiers and voltage regulator, several improvements in the ordinary FEA must be adopted.

In the followings, first, we briefly address the computation method and its mathematical background. Then, we present the results obtained numerically and their comparison with the measured ones in order to verify the precision of our approach. Finally, we describe the simulation method and the obtained results for three-phase brushless synchronous generator, and give some final remarks and conclusions.

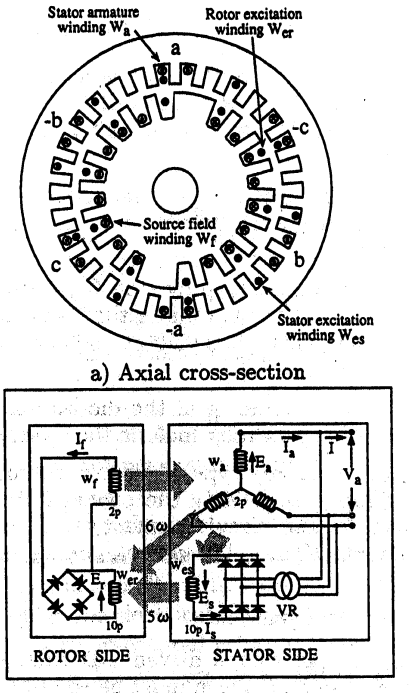

Fig. 1. Model of the analyzed brushless synchronous generator.

II. Computation Method

The electric circuit of the analyzed three-phase brushless generator with semiconductors, as can be seen in Fig. 1 is rather complex. The generator comprises four separate windings: the two-pole stator armature winding W_a and ten-pole excitation winding W_{es} on the stator side, and the two-pole source field winding W_f and ten-pole excitation winding W_{er} on the rotor side of the generator. The complexity of the electric circuits is further enhanced due to the existence of the rectifiers' circuits on both stator and rotor sides and a voltage regulator VR on the stator side. Therefore, in order to simulate the operating conditions of this generator we developed a simulation method which presents the following features:

- As the current values are unknown in advance and they are strongly dependent on the circuit parame-

Manuscript received June 3, 1998.
Hideo Yamashita, +81 824-24-7665, fax +81 824-22-7195, yama@eml.hiroshima-u.ac.jp, http://www.eml.hiroshima-u.ac.jp/

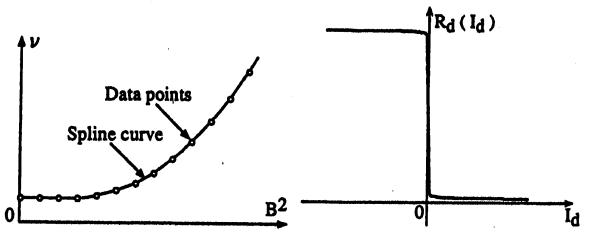

a) Spline approximation b) Diode characteristic

Fig. 2. Approximation of the ν–B^2 and $R_d(I_d)$–I_d characteristics.

ters, field distribution and operating conditions, voltage driven FEA was adopted to enable solving the magnetic field and electric circuit equations simultaneously.

- Due to the existence of magnetic circuits with saturated magnetic materials a nonlinear FEA was adopted.
- Time-periodical step-by-step FEM was employed in order to correctly evaluate the transient characteristic of the generator's voltage and current changes due to its rotation [4].
- Numerical modeling of the diodes was developed in order to successfully include them into the analysis.
- Modeling of any type of electric circuit was enabled by simply using only the connectivity patterns between various circuit elements such as resistors, inductors, DC and AC sources, condensers and diodes.

A. Governing Equations

In the voltage source driven 2-D FEA the governing system of equations which must be solved simultaneously are generated according to the Maxwell equations and the Second Kirchoff Law [5]

$$rot\,(\nu rot\boldsymbol{A}) = \boldsymbol{J_0} - \sigma(\frac{\partial \boldsymbol{A}}{\partial t} + grad\phi)\,, \qquad (1)$$

$$\frac{\partial \Phi}{\partial t} + RI_0 + L\frac{\partial I_0}{\partial t} - V_0 = 0\,, \qquad (2)$$

where $\boldsymbol{A}$ is the magnetic vector potential, $\boldsymbol{J_0}$ is the source current density vector and ϕ is the electric scalar potential. Additionally, in (2), Φ stands for the total magnetic flux, I_0 and V_0 are the source current and supplied external voltage, while R and L are the resistance and inductance of the part of electric circuit which is not included inside the finite element analysis area [5]. The coupling between (1) and (2) is enabled using the values of the source current intensity I_0 and its density vector $\boldsymbol{J_0}$, and the value of the total magnetic flux Φ.

B. Nonlinear Modeling

As can be observed in Fig. 1, inside the analysis region, two strongly nonlinear elements exists: the nonlinear magnetic materials and the rectifiers' diodes. Due to strongly nonlinear magnetic characteristic of the magnetic materials a nonlinear magnetic circuit must be considered, thus we utilized a traditional Newton-Raphson nonlinear iteration process. For modeling of the magnetic characteristic ν–B^2, a second order spline approximation was used utilizing previously available measured data as shown in Fig. 2a.

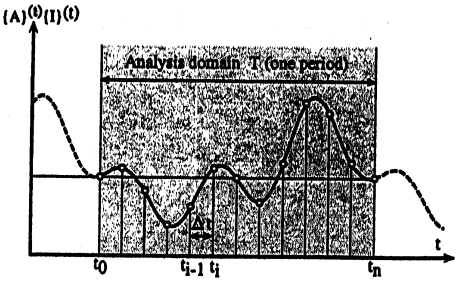

Fig. 3. Time periodical FEA using step-by-step method.

For modeling of the nonlinear switching characteristic of the rectifiers' diodes, shown in Fig. 2b, we must model the dynamic resistance of the diodes R_d according to the current changes I_d. This modeling was done according to the following empirical equations

$$R_d(I_d) = \begin{cases} \frac{1}{\sqrt{100(I_d+4.0\times10^{-10})}} & (I_d \geq 0) \\ \frac{-1}{\sqrt{-100(I_d-4.0\times10^{-10})}} + 10000 & (I_d < 0) \end{cases} \qquad (3)$$

C. Time-periodic FEA

Accurate modeling of first derivatives of currents and magnetic vector potential is very important. Due to their periodical but non-sinusoidal character they can not be simply modeled using complex representation $j\omega$, but a time discretization must be employed. In this analysis we employed the time-periodic step-by-step FEM [4] schematically shown in Fig. 3. This method enables representation of the first derivative of any time-varying variable, e.g. the phase currents, at each time step t as a function of its value at time $t - \Delta t$

$$\frac{\partial I_0^{(t)}}{\partial t} = \frac{I_0^{(t)} - I_0^{(t-\Delta t)}}{\Delta t} \qquad (4)$$

where Δt is the computation time step. Therefore, at each time step t the following system of algebraic equations is generated

$$\begin{Bmatrix}\{0\}\\\{0\}\end{Bmatrix} = \begin{bmatrix}[K]^{(t)}+[T] & [S]\\ [S]^T & [Z_R]^{(t)}+[Z_X]\end{bmatrix}\begin{Bmatrix}\{A\}^{(t)}\\\{I\}^{(t)}\end{Bmatrix} - \begin{bmatrix}[T] & [0]\\ [S]^T & [Z_X]\end{bmatrix}\begin{Bmatrix}\{A\}^{(t-\Delta t)}\\\{I\}^{(t-\Delta t)}\end{Bmatrix} - \begin{Bmatrix}\{0\}\\\{V\}^{(t)}\end{Bmatrix} \qquad (5)$$

As shown in Fig. 3, during analysis it is necessary that the values of the unknown variables coincide at the terminal points of the analyzed time domain which is usually equal to one time period, e.g. $A(t_0) = A(t_n)$. This condition enables generation of the system of algebraic equations for the entire time domain by summation of all system matrices (5) generated at each time step, respectively. Finally, according to the periodical symmetry of the model and its rotation, the generated system of linear equations, must be transformed using periodical boundary conditions, and later solved for the unknown values

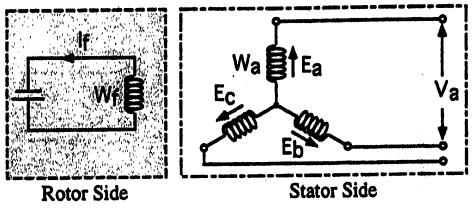

Fig. 4. Electric circuit for no-load characteristic simulation.

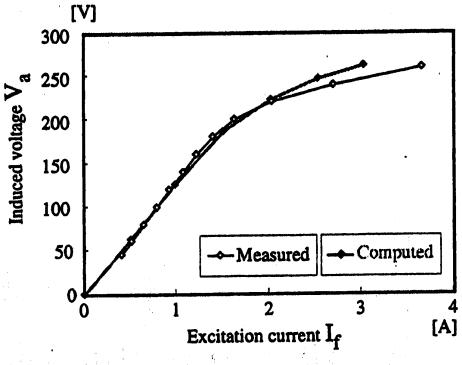

Fig. 5. Computer simulated no-load characteristic.

of the magnetic vector potential and the current values at each time step, respectively.

III. Simulation Results

A. No-load Characteristics

The electric circuit for simulation of the no-load characteristic is given in Fig. 4, while the obtained no-load characteristic is given in Fig. 5, together with the experimental data obtained by performing measurements on the modeled generator. Actually, because the magnetic characteristic of the material was unknown, these measured data were used for modeling the B–H magnetic curve, i.e. the ν–B^2 curve. The obtained computer simulation of the no-load characteristic is given in Fig. 5. As can be seen computed results are in very good agreement with the measured ones almost for the entire working area. The small discrepancy can be observed only for large values of the excitation current, which we believe, is the result of the large saturation of magnetic materials for large values of source current of the modeled generator.

B. Load Characteristics

For simulation of load characteristics of the analyzed brushless synchronous generator, the electric circuit shown in Fig. 1b was utilized. Comparing with the electric circuit shown in Fig. 4 one can easily observe that the electric circuit for simulating the load characteristics is much more complicated than the previous one. The coupling among the stator and rotor windings for these circuits is strong, and the existence of diodes and voltage regulator VR makes the computer simulation extremely complex. Several generator parameters were monitored

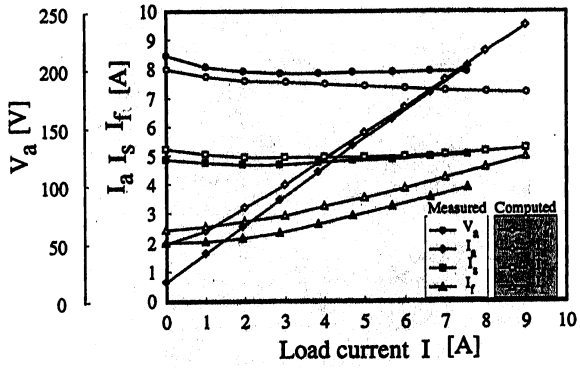

Fig. 6. Load characteristics computer simulation.

TABLE I
COMPUTATIONAL COST PER ANALYSIS

Total number of unknowns (Points + Sources) × Time Steps	Computation time
(1,635 + 10) × 360 = 592,200	about 12 hours

Silicon Graphics Indigo2 Workstation, 136 MIPS.

during simulation of the load condition, among them, the time changes and the maximum induced voltage V_a at the generator's terminals, the maximum value of the source field current I_f and the values of excitation current I_s and I_r on stator and rotor side, respectively. Figure 6 shows the obtained results of the computer simulation using time step of one electrical degree. For comparison, in the same figure the measured values are also plotted. The computed results are in very good agreement with the measured ones for almost entire working area. However, a small discrepancy between measured and computed results can still be observed especially for small values of the load current I such as for load current $I = 0$ A. We believe that this is due to the modeling method for the voltage regulator VR and neglecting its magnetic losses.

In Fig. 7, the computed distribution of magnetic flux density $\boldsymbol{B}$ using quasi-color display is shown together with flux lines at one particular time step. Additionally, in Fig. 8 the time variations of the induced voltages at the analyzed generator terminals for all three phases are presented. It is clearly visible that the induced voltage exhibits ripples which are mainly due to the fact that we neglected the skewed structure of the rotor. This should be a priority in our future research.

Finally, Table I shows the number of unknowns and the total computation time for analysis over time interval of one period utilizing nonlinear time-periodic FEA. Although the number of unknowns is rather large, we believe that the computation time of approximately 12 hours is still acceptable for such a complex analysis.

C. Analysis of High Frequency Components

To achieve a high quality of the generator's output voltage, the high frequency harmonic analysis must be performed. Additionally, due to the existence of the semi-

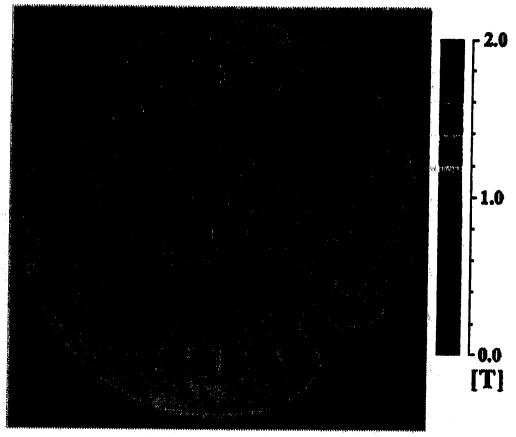

Fig. 7. Computed magnetic flux density and flux line distribution.

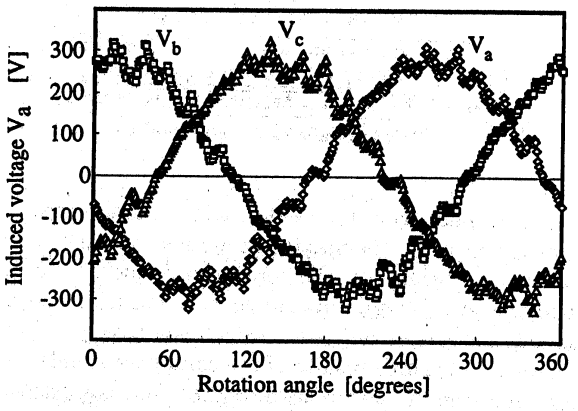

Fig. 8. Time-periodical changes of induced voltage V_a, V_b and V_c.

conductors and windings with various number of poles on stator and rotor side, we expected that the amount of high frequency components should not be neglected. Figure 9a shows the harmonic analysis of the induced voltage at the generator's terminals V_a. As can be seen, the first harmonic is dominant with very small values of other odd higher harmonics. Somehow larger values were obtained only for the 17th and 19th harmonic as a result of generator's slot distribution which agrees very well with measurements. Regarding the excitation voltage on rotor side E_r, the situation with high frequency components is totally different, as shown in Fig. 9b. In this case, the fifth and sixth components are dominant, as one can expected because stator and rotor fields are coupled with frequencies 5ω and 6ω (see Fig. 1b). Due to the existence of rectifiers, also the other high frequency components of order five and six are dominant which agrees very well with our expectations.

IV. Conclusions

In this paper, we presented a method for numerical computation and simulation of three-phase brushless synchronous generator under different operating conditions. Using voltage driven 2-D nonlinear time-periodic FEA,

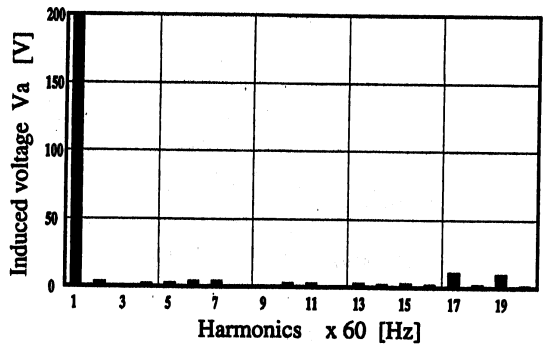

a) Induced voltage V_a

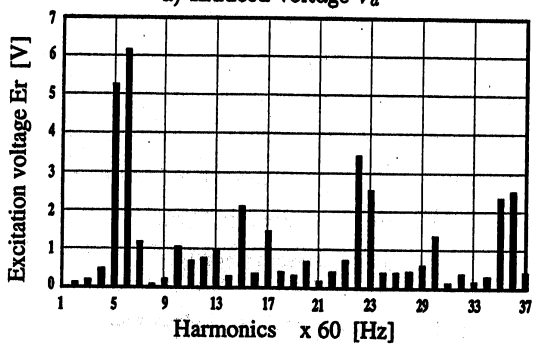

b) Rotor excitation voltage E_r

Fig. 9. Computed high frequency harmonics.

the magnetic field distribution and the induced voltage and currents were computed accurately. For modeling the diode characteristic a simple and fast empirical equation was used, while the magnetic characteristic was modeled using second order spline approximation. The computational approach was verified using experimental results obtained from a test model of brushless synchronous generator. The achieved agreement between experimental results and computed results was very good.

References

[1] T. Nakata and N. Takahashi, "Direct Finite Element Analysis of Flux and Current Distributions under Specified Conditions," *IEEE Transaction on Magnetics*, MAG-18, No.2, pp.325, 1988.

[2] H. Yamashita, E. Nakamae, and H. Yoshimoto, "Electric Network Analysis Including a Region of Finite Element Analysis," *IEEE Transaction on Magnetics*, MAG-23, No.5, pp.3578-3580, 1987.

[3] K. Inoue, H. Yamashita, E. Nakamae, and T. Fujikawa, "Brushless Self-Excited Three-Phase Synchronous Generator without Exciter," *Transaction on IEE of Japan*, D.112, No.6, pp.596, 1992. (in Japanese)

[4] T. Hara, T. Naito, and J. Umoto, "Field Analysis of Corona Shield Region in High Voltage Rotating Machines by Time-Periodic Finite Element Method: I. Numerical Calculation Method," *Transaction on IEE of Japan*, D.102, No.7, pp.423, 1982. (in Japanese)

[5] V. Cingoski and H. Yamashita, "Analysis of induction skull melting furnace by edge finite element method excited from voltage source," *IEEE Transaction on Magnetics*, Vol. 30, No.5, pp.3459-3462, 1994.